PHYSICAL REVIEW A **76**, 013411 (2007)

# High-brilliance free-electron-laser photoionization of $N_2$: Ground-state depletion and radiation-field-induced modifications

A. Föhlisch,[*] M. Nagasono,[†] M. Deppe, E. Suljoti, F. Hennies, A. Pietzsch, and W. Wurth
*Institut für Experimentalphysik, Universität Hamburg, Luruper Chaussee 149, 22761 Hamburg, Germany*

(Received 5 February 2007; published 19 July 2007)

Valence photoionization of $N_2$ has been performed with high-brilliance vacuum ultraviolet radiation at $h\nu = 38.5 \pm 0.2$ eV from the free-electron laser at Hamburg (FLASH). As a function of fluence, saturation of photoionization occurs due to the depletion of the ground-state molecular target within each femtosecond radiation pulse. With increasing fluence, the vibrational envelope of the valence photoionization spectral distribution experiences radiation-field-induced changes.

DOI: 10.1103/PhysRevA.76.013411 PACS number(s): 33.80.Rv, 33.60.Cv, 33.70.−w, 33.90.+h

With photoelectron spectroscopy, the electronic structure of matter is explored and the potential energy surfaces of molecules can be mapped via the vibrational fine structure of spectral states [1,2]. The homonuclear dimer $N_2$ is a prototypical molecular system, with $D_{\infty h}$ symmetry, where with ultraviolet photoelectron spectroscopy the molecular $2\sigma_u$, $1\pi_u$, and $3\sigma_g$ orbitals can be investigated; they are denoted spectroscopically as the $\Sigma_u^+$, $\Pi_u$, and $\Sigma_g^+$ states, respectively [1]. The photon-energy-dependent total and partial-shell photoionization cross sections have been reported [4]. The vibrational progression of the $\Sigma_u^+$, $\Pi_u$, and $\Sigma_g^+$ states varies due to the different changes of the internuclear equilibrium distance resulting from the valence ionization of the $2\sigma_u$, $1\pi_u$, and $3\sigma_g$ orbitals, according to the Franck-Condon principle [2].

In this paper, we discuss the valence photoionization of $N_2$ measured with extreme ultraviolet radiation of 38.5 eV from the free-electron laser at Hamburg (FLASH) with unprecedented peak brilliance [5]. We observe significant deviations in the photoionization spectral distributions (intensity and shape) as a function of fluence. This is attributed to the depletion of the ground-state molecular target within each individual femtosecond radiation pulse, but also to the influence of the electromagnetic peak field strength on the molecular potential energy surfaces.

Experimentally, photoelectron spectra of $N_2$ have been measured with the gigawatt peak power of the free-electron laser in Hamburg which provides extreme ultraviolet and soft x-ray radiation, between 12 and 200 eV [5]. FLASH was operated at a photon energy of $h\nu = 38.5 \pm 0.2$ eV with 2 Hz macropulse repetition rate, each macropulse containing eight micropulses of 25 fs duration and 1 $\mu$s temporal distance [5]. Due to the self-amplified spontaneous emission (SASE) process a shot-to-shot fluctuation of the photon pulse energy between 0 and 18 $\mu$J occurred and was monitored. The radiation was guided through the monochromator beamline PG2 [6] and a 700 nm Al filter 530 mm upstream of the focal point. Thus the high harmonic radiation of the self-amplified spontaneous emission undulator [7] was suppressed, and the contamination to the primary radiation at $h\nu = 38.5 \pm 0.2$ eV was below $5 \times 10^{-9}$ (computed from x-ray optical constants [8]). The Al filter and the beamline optics (all coated with high-density carbon) gave 10% transmission of the primary radiation due to the combined beamline [6] and filter transmission [8], thus yielding pulse energies up to 1.8 $\mu$J. The experimentally determined interaction area in our ultrahigh-vacuum experimental system (base pressure $< 2 \times 10^{-10}$ mbar) was 200 $\mu m^2$, leading to an electric peak field strength on the order of 1 V/Å during the 25 fs pulse duration. As depicted in Fig. 1, $N_2$ at $7 \times 10^{-6}$ mbar was introduced to the experimental chamber via a copper capillary with an inside diameter of 200 $\mu$m at 1 mm distance from the focal point. The intensity of the transmitted radiation per pulse was determined shot to shot by converting the xuv radiation in a cerium-doped yttrium aluminum garnet (Ce:YAG) crystal into visible light detected by a gated charge-coupled device (CCD) camera, synchronized to the 2 Hz macrobunch repetition rate. This signal was calibrated against the established photon numbers measured with a gas-monitor detector [9,10]. The photoelectron spectra were measured at magic angle detection geometry relative to the linearly polarized radiation with a hemispherical electron energy analyzer (Gammadata SES 2002) at a pass energy of 100 eV and an entrance slit size of 300 $\mu$m. Here, the spectral image was also recorded shot to shot by a second gated CCD camera, also synchronized to the 2 Hz macrobunch repetition rate. Thus, the shot-to-shot images of these two

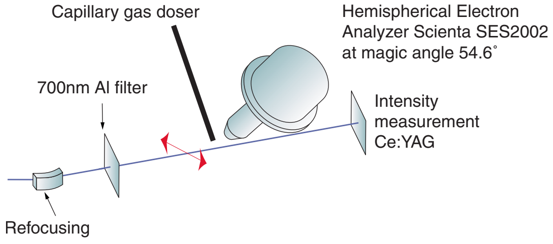

FIG. 1. (Color online) Free-electron laser (FEL) radiation is focused and spectrally filtered onto the $N_2$ gas target introduced into the ultrahigh-vacuum experimental chamber by a capillary. Photoelectrons are detected by a hemispherical electron analyzer at magic angle detection geometry relative to the linearly polarized radiation with $h\nu = 38.5 \pm 0.2$ eV photon energy. On a shot-to-shot basis, the incident photon pulse energy and the resultant photoelectron spectrum were recorded.

---

[*] Corresponding author. alexander.foehlisch@desy.de
[†] nagasono@spring8.or.jp

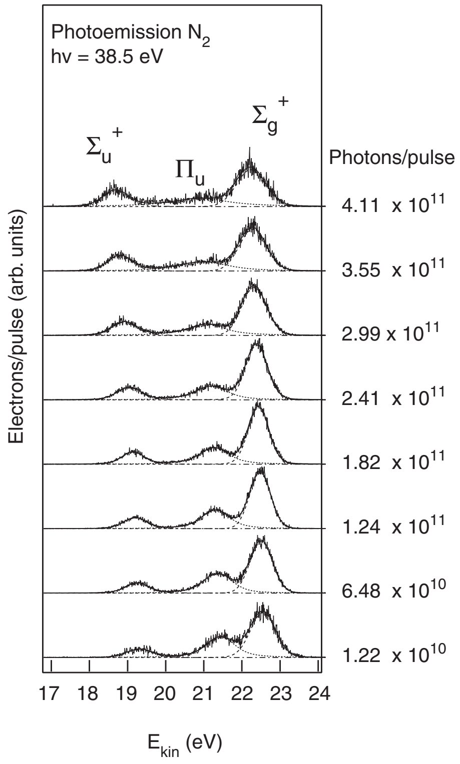

FIG. 2. Valence photoelectron kinetic energy distribution curves of $N_2$ at $7 \times 10^{-6}$ mbar and curve fits as a function of photon number per 25 fs free-electron-laser radiation pulse at photon energy $h\nu = 38.5 \pm 0.2$ eV in the 200 $\mu m^2$ interaction zone. Normalized to unit area.

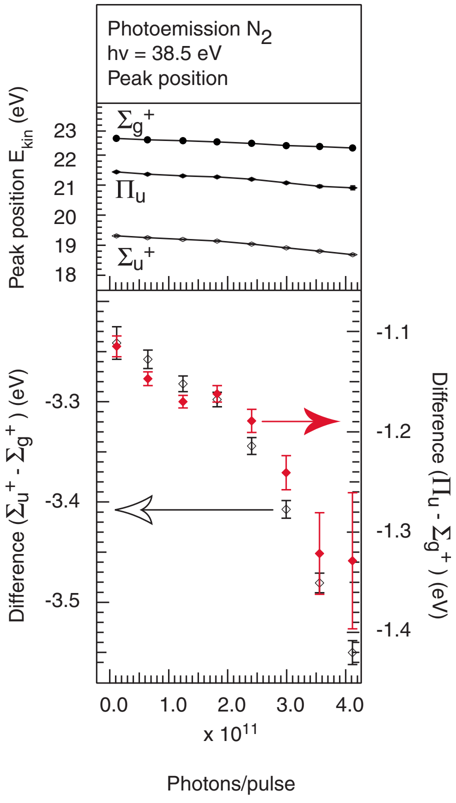

FIG. 3. (Color online) Photon pulse energy dependence of the peak positions of the $\Sigma_g^+$, $\Pi_u$, and $\Sigma_u^+$ states. Upper panel, absolute values; lower panel; shift of the $\Pi_u$ and $\Sigma_u^+$ states relative to the $\Sigma_g^+$ state.

CCD cameras provide photoelectron spectral intensity and photon pulse energy for each pulse.

In Fig. 2 the photoelectron energy distribution curves of the $N_2$ valence states per femtosecond radiation pulse (25 fs) are shown as a function of the incident photons per pulse. Here, the full range of all encountered photon pulses has been binned into eight equally wide regions, each denoted by their respective mean photon number. For photon numbers per pulse between $1.22 \times 10^{10}$ and $4.11 \times 10^{11}$, we observe the $\Sigma_g^+$, $\Pi_u$, and $\Sigma_u^+$ spectral states. As the full SASE first harmonic is used without further monochromatization, we observe in the spectral width the statistical bandwidth envelope of the SASE first harmonic averaged over many pulses [7]. In particular, we observe a variation of the relative intensities and shifts in the peak positions partly accompanied by changes in peak shapes. The statistics of the spectra vary, reflecting the probability distribution of SASE for each given photon pulse energy [7]: As more intense photon pulses occur less often our photoelectron spectra toward high photon pulse energies show larger statistical noise. To quantify our experimental findings we have performed a curve-fitting analysis (Fig. 2) of the experimental data. All spectral states ($\Sigma_g^+$, $\Pi_u$, and $\Sigma_u^+$) can be fitted with Voigt line profiles representing the vibration envelope of each electronic state and the 0.4 eV bandwidth of each exciting FEL radiation pulse. As directly seen in Fig. 2 and quantified in Fig. 3, upper panel, all spectral states show a shift toward lower kinetic energy with increasing photon pulse energy due to space charge. In addition to this general trend, the energy shifts of the $\Sigma_g^+$, $\Pi_u$ and $\Sigma_u^+$ vary as a function of the photon pulse energy as seen in the lower panel of Fig. 3.

This relative variation in peak maxima cannot be explained as due to space charge. Space charge should affect all states equally, in addition to the known modifications in angular distribution giving small modifications in intensity at fixed detection geometry [3]. Thus, the observed variation in peak maxima must be related to a change of peak shape, i.e., the underlying vibrational progression within each state. Thus we also show in Fig. 4 the evolution of the full width at half maximum (FWHM) of each state as a function of photon pulse energy. Whereas the $\Sigma_g^+$ and $\Sigma_u^+$ peaks show little change in their FWHMs, the $\Pi_u$ state broadens notably above $2.99 \times 10^{11}$ photons per pulse. Finally, we present in Fig. 5 the integral and state-resolved spectral intensities as a function of photon pulse energy. In each figure, the error bar corresponds to the standard deviation.

In a first step, we relate the experimentally observed photon pulse energy dependence to the known subshell photoionization cross sections of $N_2$ ($\Sigma_g^+$, 4 Mb; $\Pi_u$, 8 Mb; $\Sigma_u^+$, 2 Mb [4]) based on a saturation formula [9]

$$I_{PE} = C(1 - e^{-\sigma I_{h\nu}/A}) \tag{1}$$

effectively describing how the probing volume is depleted of $N_2$ molecules in the electronic ground state with increasing photon number per pulse. Here $I_{PE}$, $\sigma$, $I_{h\nu}$, and $A$ denote

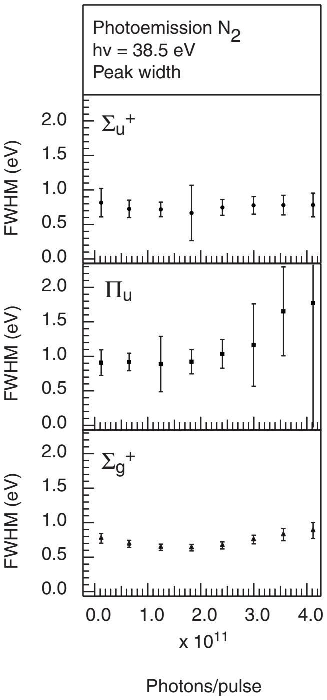

FIG. 4. Photon pulse energy dependence of the full width at half maximum (FWHM) of the $\Sigma_g^+$, $\Pi_u$, and $\Sigma_u^+$ states.

photoelectron intensity, subshell photoionization cross section, photons per pulse, and the monitored interaction area, respectively, and $C$ contains the initial number of molecules in the interaction region as well as the transmission of the electron analyzer. Having only $C$ as a free parameter, we can describe the saturation behavior for all spectral states as a consequence of direct single-photon photoemission. The photoionization of the three $N_2$ valence orbitals $2\sigma_u$, $1\pi_u$, and $3\sigma_g$ with linearly polarized radiation involves different subsamples of $N_2$ molecules with different spatial orientations. The subsamples with a higher photoionization cross section show already at lower photon pulse energy ground-state depletion, which causes the experimentally observed state-resolved dependence of photoionization events as a function of photon number per pulse.

Let us now turn to our observations regarding peak shapes (Fig. 4) and peak positions (Fig. 3). Neither the relative shifting of spectral peaks nor the broadening of the $\Pi_u$ state (the molecular $1\pi_u$ orbital) above $2.99\times10^{11}$ photons per pulse, which is not observed in the $\Sigma_g^+$ and $\Sigma_u^+$ states, representing ionization from the $2\sigma_u$ and $3\sigma_g$ orbitals (Fig. 4), can be explained by a simple model of direct photoionization and electronic ground-state depletion in the sample volume. Likewise, space charge effects can be excluded, as they would influence all three spectral states. Thus, we have to consider the fact that, during the 25 fs radiation pulses, the $N_2$ molecular target is exposed to an electric peak field strength up to 1 V/Å. Our observations of significant broadening of the $\Pi_u$ state (Fig. 4), as well as the different shifting of the $\Sigma_g^+$, $\Pi_u$, and $\Sigma_u^+$ states (Fig. 3) toward high photon pulse energies, could be due to a radiation-field-induced modification of the ground state and the valence-ionized final-state potential energy surfaces [11–13]. The $\Pi_u$ state has, according to the Franck-Condon principle [2], a high vibrational progression due to the large change of internuclear equilibrium distance between the photoionization initial and final states, which is in contrast to the $\Sigma_g^+$ and $\Sigma_u^+$ states. Thus, we believe that our observations are the result of modified vibrational progressions underlying each spectral state, changing both peak width and peak position (maximum) of each vibrational envelope.

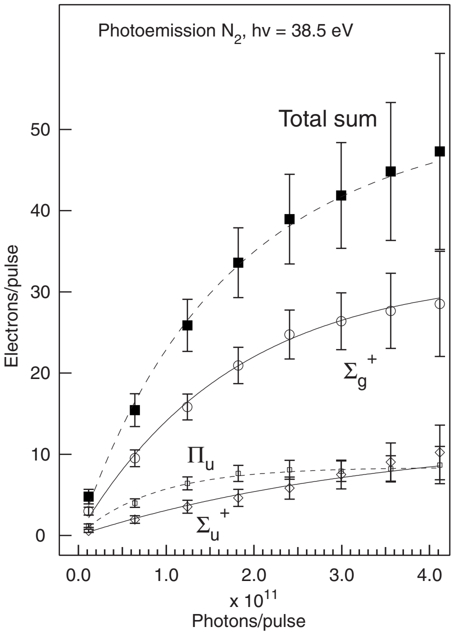

FIG. 5. Integral and state-resolved photoelectrons per photon pulse from least-squares curve fitting of spectral data in Fig. 2. The dependence on the incident photon number per pulse is fully described by a depletion of the molecular ground state, described with the saturation expression Eq. (1).

In summary, we have measured in gaseous $N_2$ photoionization with the unprecedented excitation brilliance of ultraviolet radiation from the free-electron laser at Hamburg. The $N_2$ valence spectral intensity as a function of fluence is fully described by the subshell photoionization cross sections in combination with a depletion of the photoionization probe volume from ground-state $N_2$. In addition, at large fluences, the relative peak positions and envelopes of spectral states change, which we interpret as a field-induced modification of the potential energy surfaces detected with photoelectron spectroscopy.

We gratefully acknowledge the scientific and technical staff of the FLASH facility, in particular V. Kocharyan, B. Fominykh, V. Rybnikov, K. Rehlich, and R. Treusch. This work was supported by the German Ministry of Education and Research through Grants No. 05 KS4GU1/8 and No. 05 KS4GU1/9 and the Helmholtz Joint Research Center "Physics with Coherent Radiation sources."

[1] K. Kumura, S. Katsumata, Y. Achiba, T. Yamazaki, and S. Iwata, *Handbook of HeI Photoelectron Spectra of Fundamental Organic Molecules* (Japan Scientific Societies Press, Tokyo, 1981).

[2] G. Herzberg and J. W. T. Spinks, *Molecular Spectra and Molecular Structure* (Prentice-Hall, New York, 1966), Vol. 1.

[3] S. Passlack, S. Mathias, O. Andreyev, D. Mittnacht, M. Aeschlimann, and M. Bauer, J. Appl. Phys. **100**, 024912 (2006).

[4] E. W. Plummer, T. Gustafsson, W. Gudat, and D. E. Eastman, Phys. Rev. A **15**, 2339 (1977).

[5] V. Ayvazyan *et al.*, Eur. Phys. J. D **37**, 297 (2006).

[6] M. Martins, M. Wellhöfer, J. T. Hoeft, W. Wurth, J. Feldhaus, and R. Follath, Rev. Sci. Instrum. **77**, 115108 (2006).

[7] S. Düsterer *et al.*, Opt. Lett. **31**, 1750 (2006).

[8] B. Henke, E. Gullikson, and J. Davis, At. Data Nucl. Data Tables **54**, 181 (1993).

[9] M. Richter *et al.*, Appl. Phys. Lett. **83**, 2970 (2003).

[10] J. Feldhaus *et al.*, J. Phys. B **38**, S799 (2005).

[11] K. Yamanouchi, Science **295**, 1659 (2002).

[12] *Atoms in Intense Laser Fields*, edited by M. Gavrila (Academic, New York, 1992).

[13] *Molecules in Intense Laser Fields*, edited by A. D. Bandrauk (Dekker, New York, 1994).